Evaluation of the Rotating-Frame Relaxation (T 1ρ) Filter and Its Application in Metabolomics as an Alternative to the Transverse Relaxation (T 2) Filter

Elena Piersanti, Lamya Rezig, Fabrice Tranchida, Wael El-Houri, Seidou Abagana, Mylène Campredon, Laetitia Shintu, Mehdi Yemloul

HAL Id: hal-03655575
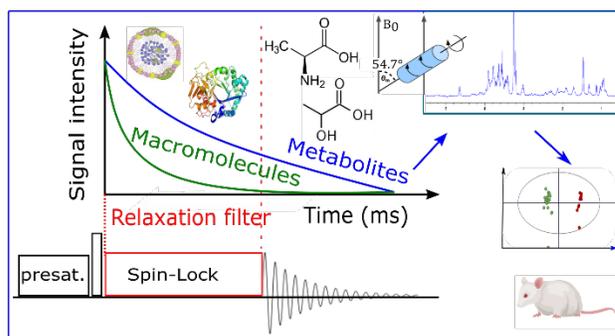https://amu.hal.science/hal-03655575

Submitted on 29 Apr 2022

Evaluation of the rotating-frame relaxation ($T_{1\rho}$) filter and its application in metabolomics as an alternative to the transverse relaxation (T_2) filter

Elena Piersanti[iD], Lamya Rezig, Fabrice Tranchida, Wael El-Houri, Seidou M. Abagana, Mylène Campredon, Laetitia Shintu[iD] and Mehdi Yemloul[iD]*.

Aix Marseille Univ, CNRS, Centrale Marseille, iSm2, Marseille, France.

ABSTRACT: NMR-based metabolomic studies commonly involve the use of T_2-filter pulse sequences to eliminate or attenuate the broad signals from large molecules and improve spectral resolution. In this paper, we demonstrate that $T_{1\rho}$ filter-based pulse sequence represents an interesting alternative since it allows the stability and the reproducibility needed for statistical analysis. The integrity of the samples and the stability of the instruments were assessed for different filter durations and amplitudes. We showed that the $T_{1\rho}$ filter pulse sequence did not induce sample overheating for a filter duration up to 500 ms. The reproducibility was evaluated and compared with T_2-filter in serum and liver samples. The implementation is relatively simple and provides the same statistical and analytical results as those obtained with the standard filters. Regarding tissues analysis, since the duration of the filter is that of the spin-lock, the synchronization of the echo delays with the Magic Angle Spinning (MAS) rate is no longer necessary as for T_2 based filter sequences. The results presented in this article aim at establishing a new protocol to improve metabolomic studies and pave the way for future developments on $T_{1\rho}$ alternative filters, on liquid and HR-MAS NMR experiments.

Introduction

Serum and plasma are among the most common samples analysed by NMR-based metabolomics.[1,2] To limit metabolite intensity variations, sample collection and preparation have to be tightly monitored, reducing the number of needed pre-treatment steps. Therefore, purification steps such as protein removal from plasma or tissue samples, are usually not performed before NMR analysis. This leads to the acquisition of complex NMR spectra, containing signals from macromolecules (proteins, lipoproteins) overlapping the signals of metabolites of interest. Several spectral editing NMR sequences have been proposed to suppress or reduce the signal of these macromolecules in order to get a better visualization of the metabolite signals. In general, the complete elimination or the attenuation of macromolecule signals exploits the variation of the spin relaxation parameters using relaxation-weighted experiments, in which macromolecule signals, with short relaxation times, vanish. In the established metabolomic protocols, the only filter used is the T_2 based one with the CPMG pulse sequence.[3] One drawback of this relaxation filter is the echo modulation arising from the homonuclear scalar coupling, that typically leads to negative signals with loss of intensity on CPMG filtered spectra,[4] and which is not completely refocused by the multiple CPMG block even when the inter-pulse frequency ($1/\tau$, where τ is the inter-pulse delay)

is much larger than J coupling values ($1/\tau >>> J$).[5-6] Moreover, the use of short inter-pulse delays requires several cycle repetitions to reach the suited filter length, causing the heating of the samples. Several strategies have been proposed to overcome these issues.[7-11] For example, S. Viel and co-workers proposed a strategy based on multiple quantum-filtered pulse sequence, in which, the complete cancelation of the modulations due to the scalar coupling is obtained by summing the zero-quantum filtered and double-quantum filtered amplitudes.[12] However, the proposed approaches so far are limited to scalar coupled two-spin systems and do not allow a broad-scale application. More recently, Aguilar and co-workers[13] formally demonstrated that the effect of the so-called "Perfect Echo" sequence, proposed by Takegoshi *et al.*[14], is not limited to AX spin systems, but could be extended to multiple coupled spins. Hence, CPMG with a 90°_y refocusing pulse at the midpoint of a double spin-echo was introduced as PROJECT (Periodic Refocusing of J Evolution by Coherence Transfer) and was successfully used in metabolomics, particularly for HR-MAS NMR-based studies of tissue samples where long inter-pulse delays must be used for rotor synchronization.[4, 15-16] Despite all these improvements, spin coherence transfer, that occurs for any CPMG schemes, means that T_2 cannot be considered as accurate for individual spins and may introduced problems for absolute quantification.[17] When

dealing with a proton spectrum involving many multiplets, a simple alternative can be used, the so-called relaxation time in the rotating frame, $T_{1\rho}$, which is known to carry similar information as T_2. It is often measured from the decay of the nuclear magnetization locked in the transverse plan by a radio frequency field using the spin-lock technique described by Redfield.[18] In solution, the relaxation time $T_{1\rho}$ has a very close value (if not identical) to the transverse relaxation time T_2 for small metabolites. An immediate advantage of this relaxation time is that there is no precession during the evolution period of the magnetization. This results in the absence of modulations related to possible scalar J couplings. Although similar results are obtained using T_2 or $T_{1\rho}$ filters, and, despite the advantages of $T_{1\rho}$, there is no application on mixture analysis or in metabolomics.[19] Conversely, it is widely used in solid-state NMR[20] and MRI[21-25] to improve the contrasts of the images, and several developments have been undertaken to mitigate the adverse effect of spin-locking[26] such as adiabatic rf pulses,[27-28] or phase cycling methods[28] for simultaneous B_1 rf and B_0 field inhomogeneity compensation.[29-30] In liquid-state, $T_{1\rho}$ filtering is usually used in NOE (Nuclear Overhauser Effect) and STD (Saturation Transfer Difference) experiments in protein-ligand interaction studies for the elimination of protein signals.[31] There are many potential fields of application reported in the literature, particularly in the study of complex and heterogeneous biological systems in solution and HR-MAS NMR such as lipid bilayers,[32] nanodiscs,[33] membrane proteins[34] and bicelles.[35 36 37 38] For example, the use of lab and rotating frame experiments such as INEPT and CP is well described for HR-MAS and solid-state NMR for the characterization of the membrane topology and dynamic properties of full-length rabbit cyt-b5 in a membrane environment,[39] and more recently, the in $situ$ determination of molecular structure of cartilage.[40] In HR-MAS spectroscopy, it has been used in several systems[41] but has never been performed and assessed in the context of metabolomics. Hence, the developments, as is the case of solid-state NMR and MRI, are very limited. Recently, H. Tang et al.[42] discussed T_1-, $T_{1\rho}$-, and T_2-filtered 1D and 2D experiments by comparing spectra and relaxation times for different metabolites on blood plasma, but the relevance of the $T_{1\rho}$ filter as a metabolomic tool (from spectral acquisition to statistical analysis) was not discussed. In this paper, we evaluated the implementation of the $T_{1\rho}$ filter for the metabolomic analysis of liquid and semi-solid samples (rat sera and livers), we showed that it led to statistical results identical to those obtained with the T_2 filter (CPMG and PROJECT pulse sequences). We also showed that $T_{1\rho}$ filter is suitable for metabolomic studies with a simple implementation and minimal parameter optimization, and that it does not affect the sample integrity since it does not induce overheating under the experimental conditions of metabolomics.

Materials & Methods

Samples
The collection of the samples used for this study is detailed in our previous publications.[43-44] Serum and liver samples were collected from rats that have received two different diets: (i) a standard diet (control group – C) (ii) High Fructose and Saturated fatty acids diet (HFS group). The distribution of the groups is given in **SI.1.** Animal protocols were approved by the Animal Ethics Committee of the Faculty of Pharmacy of Aix-

Marseille University (Marseille, France) and in agreement with the guidelines of the French Ministry of Food and Agriculture. The samples were stored at –80°C until analysis.

Serum samples were prepared using 200 μl of serum mixed with 400 μl of 0.9 g·L^{-1} saline solution (in D_2O). Regarding tissue samples, about 15 mg of liver tissue was placed into a 30 μl cylindrical disposable insert and 10 μl of D_2O were added. The insert was then placed into an 80 μl 4 mm ZrO_2 HR-MAS rotor.

NMR recording conditions
Three pulse sequences were implemented: (i) a standard Carr−Purcell−Meiboom−Gill (CPMG) NMR spin echo sequence from the Bruker pulse program library, preceded by a water presaturation pulse during a relaxation delay ([presat-90°-(τ-180°-τ)n]); (ii) a standard $T_{1\rho}$ sequence, also preceded by a water presaturation pulse during the relaxation delay (Presat - 90°$_\phi$-(SL)$_{\phi\pm90°}$]), (the pulse sequence and implementation details are given in **SI.1**); (iii) the presaturated PROJECT sequence ([presat- 90°-(τ-180°-τ-90- τ-180- τ-)n]) from Aguilar et al.[13], used for HR-MAS experiments. The filter duration was adjusted manually to remove the macromolecules signals. The spinlock duration was set as equal to the overall echo time duration of the CPMG sequence ($i.e.$ 480 ms and 100 ms for liquid and HR-MAS, respectively). The modification and the adjustment of the filter duration are very simplified for $T_{1\rho}$-weighted sequence and do not require any calculation as is the case for T_2-based sequences for which the inter-pulse delays and the number of loops must be taken into account to obtain the desired duration. All the NMR datasets were processed with the in-built software TOPSPIN 3.6 version (Bruker BioSpin, Germany).

**For liquid-state NMR**, the experiments were performed at 293 K on a Bruker AVANCE III spectrometer operating at 600 MHz for ^{1}H frequency equipped with a triple resonance high-resolution probe producing pulse field gradients with a maximum strength of 60 G·cm^{-1}. The CPMG and $T_{1\rho}$ weighted spectra of serum were acquired using 64 scans with 16 dummy scans, the 90° hard pulse length was 9.5 μs at 18 Watts and a relaxation delay of 5 sec during which a continuous wave for water suppression was applied with a power level of 3.2 10^{-5} Watts $\left(\frac{\gamma B_1}{2\pi} = 32\ Hz\right)$. For the CPMG, the inter-pulse delay was set to 200 μs with $n=1200$ $loops$ leading to a total filter length of 480ms. The same filter length was used for the $T_{1\rho}$ spectra by adjusting the spin-lock pulse labelled "$p3$" in the pulse sequence (see **SI.2.**). For both experiment, the spectral width was set to 6000 Hz and sampled with 32768 data points leading to the acquisition time of 2.27 sec and a total experiment time of 10 minutes.

**For HR-MAS NMR spectroscopy**, the experiments were carried out on a Bruker AVANCE III spectrometer operating at 400 MHz for ^{1}H frequency equipped with a ^{1}H/^{13}C/^{31}P HR-MAS probe. All spectra were acquired at 277 K.
The CPMG, PROJECT and $T_{1\rho}$ weighted spectra of liver were acquired using 128 scans with 16 dummy scans, the 90° hard pulse length was 10 μs at 10 Watts power level and a relaxation delay of 2 sec during which water suppression with a power level of 3.2 10^{-5} Watts $\left(\frac{\gamma B_1}{2\pi} = 64\ Hz\right)$. For CPMG and PROJECT, the inter-pulse delay had to be synchronized with the two MAS spinning periods used in this study, $\tau = 1$ ms and

250μs for $\nu_{Rotation} = 1000$ Hz and 4000 Hz, respectively.[4][45] The filter length was 100ms. To reach this length, it is necessary to take into account the number of inter-pulse delays inside the loops of the two sequences, two for CPMG and four for PROJECT. The distribution of these parameters is summarized in **Table 1**. Again, the same filter length was used for the $T_{1\rho}$ spectra without any calculation by adjusting the spin-lock pulse "p3". For each experiment, the spectral width was set to 4500 Hz and sampled with 32768 data points leading to the acquisition time of 2.26 sec and a total experiment time of 10 minutes.

Table 1. The parameters τ (inter-pulse delays) and n (number of loops) used for CPMG and PROJECT to obtain a filter length of 100ms for two MAS rates (1000Hz and 4000HZ)

$\nu_{Rotation}$	CPMG (τ-180°-τ)n	PROJECT (τ-180°-τ-90- τ-180- τ-)n
1000 Hz	$\tau = 1$ m / n = 50	$\tau = 1$ m / n = 25
4000 Hz	$\tau = 250$ us / n = 200	$\tau = 250$ us / n = 100

For the relaxation times measurement, the standard pulse sequences and Bruker Dynamic Center procedure were used to record and fit the evolution of the signals as a function of the filters durations. For each sequence, the same parameters, described above, were used and the filter duration were incremented from 10 ms to 1 sec, using 12 points. For the $T_{1\rho}$ measurement, a sequence using two channels with two carrier frequencies, the first for water presaturation and the second placed at 2,2 ppm centred on the peaks of interest to avoid the offset effects. Above 2000 Hz, we observed that the measured $T_{1\rho}$ were insensitive to the position of the carrier frequency when it was on the peak of water (no offset effect).

Statistical analysis
The ^{1}H NMR spectra were directly exported to AMIX software (Bruker BioSpin GmbH, Karlsruhe, Germany) and divided into 0.001 ppm-width buckets. In order to remove effects of possible variations in the water suppression efficiency, the region of the water signal between 4.7 and 5.2 ppm was discarded. The obtained dataset (X-matrix) was then normalized to the total spectrum intensity and scaled to Unit-Variance (UV) or using Pareto scaling and imported to SIMCA P-14 software (Umetrics, Umeå, Sweden).
Orthogonal Partial Least Square - Discriminant Analyses (OPLS-DA) were then applied to the X-matrix, in order to discriminate between C and HFS groups.[46-47] The robustness of each discriminant model was then validated using a permutation method, for which 1000 OPLS-DA random models were built with an increase percentage of permutated values in the Y-matrix. For each random model, the goodness-of-fit, R^2_Y, and the predictive parameter, Q^2_Y, were calculated. The highest the Q^2, the more the model can be considered as predictive. In model systems, Q^2 are high typically > 0.7 or 0.8 for predictive models. For biological samples, as in this case, it is different. The inter-individual variability among biological samples is quite regular and therefore the overall changes are weak between different groups, therefore we considered that a predictive model is statistically robust for Q^2_y value ≥ 0.4.[48-49]
The one-way ANOVA (ANalysis Of VAriance) of the Cross-Validated (CV) predictive residuals was also calculated for each model.

Results and Discussion

Impact of $T_{1\rho}$ filter on sample heating
Some studies involving the $T_{1\rho}$ filter evoke a problem of sample heating during the application of an excessive and long spin-lock.[50-51] This effect is inherent to the nature of *rf* pulse and due to its electric component. We first evaluated this aspect using a methanol sample, which served as a molecular thermometer, to measure the actual temperature before and after the application of a 480 ms spin-lock of different amplitudes, *i. e. 2000 Hz, 4000 Hz and 5000 Hz*. For each amplitude, three methanol spectra were recorded using a one pulse sequence, after 1, 8, 64 and 128 dummy scans. The results are reported in **SI.3**. The recorded temperatures show the same small increase as for the CPMG pulse sequence, less than 0.2°C, regardless of the number of used dummy scans. The use of $T_{1\rho}$ for this kind of systems still safe but obviously, for solid state NMR studies, the amplitudes are relatively high and may disturb the samples, for example the micelle organization, protein folding and other systems including magnetically-aligned samples.[52][53][54]

Spin-lock amplitude
Conventionally the spin-lock pulse is performed by a continuous *rf* wave with an appropriate amplitude that avoids the shift between the carrier frequency and the resonance frequencies ("offset effect") and unsuitable power deposition due to excessive amplitude. Five spectra of serum were recorded with CPMG filter using two inter-pulse delays (200 μs and 600 μs) and $T_{1\rho}$ filter with different spin-lock intensities expressed as $\frac{\gamma B_1}{2\pi}$ (2 kHz, 4 kHz and 5 kHz). **Figure 1** represents the 480 ms T_2- and $T_{1\rho}$-edited proton spectra with the carrier frequency at 4.7 ppm (water frequency, also used for presaturation). The first finding was that the same filtration effect was retrieved whatever the sequence used (**Figure 1a**). However, the three $T_{1\rho}$ spectra obtained with different B_1 showed expected differences due to the offset effect.[55] Indeed, around the carrier frequency, the integrals of the signals remained unchanged when B_1 amplitude increased (**Figure 1b**), while the integrals of the peaks at the edges of the spectra increased (**Figure 1c**). Moreover, we observed a decrease of the resolution when increasing B_1 (therefore of the nutation frequency, $\nu_1 = \frac{\gamma B_1}{2\pi}$) leading to a broadening of the width at half-height of the creatine peak (singlet at 3.03 ppm) (**Figure 1a**). This trend was identical for the CPMG sequence, the resolution obtained with an inter-pulse delay of 600 μs, i.e. a CPMG pulse frequency ($\nu_{CPMG} = \frac{1}{4\tau}$, with τ the inter-pulse delay of the CPMG block) of 416.66 Hz, was higher than for the one obtained with an inter-pulse delay of 200 μs, i.e. a CPMG pulse frequency of 1250 Hz. This effect is summarized in Table SI. 4. The best resolution is obtained with $T_{1\rho}^{2kHz}$ but it is obvious that with this power the spectral coverage is not optimal to avoid offset effects. With the $T_{1\rho}^{5kHz}$, two disadvantages add up: i) the power that could be excessive, and ii) the decrease of resolution. The $T_{1\rho}^{4kHz}$ seems to be, for our study, the better amplitude that allows equalling the resolution of the $CPMG_{600\mu s}^{416\,Hz}$ sequence (see **SI. 4.**). However, the latter cannot be used since the inter-pulse delay do not allow the refocusing of the modulations due to scalar couplings as shown in **Figure 1** with the negative doublet at 4.65 ppm. In liquid-state metabolomic studies, with the commonly used CPMG filter ($CPMG_{200\mu s}^{1,25kHz}$) this effect is limited and invisible.
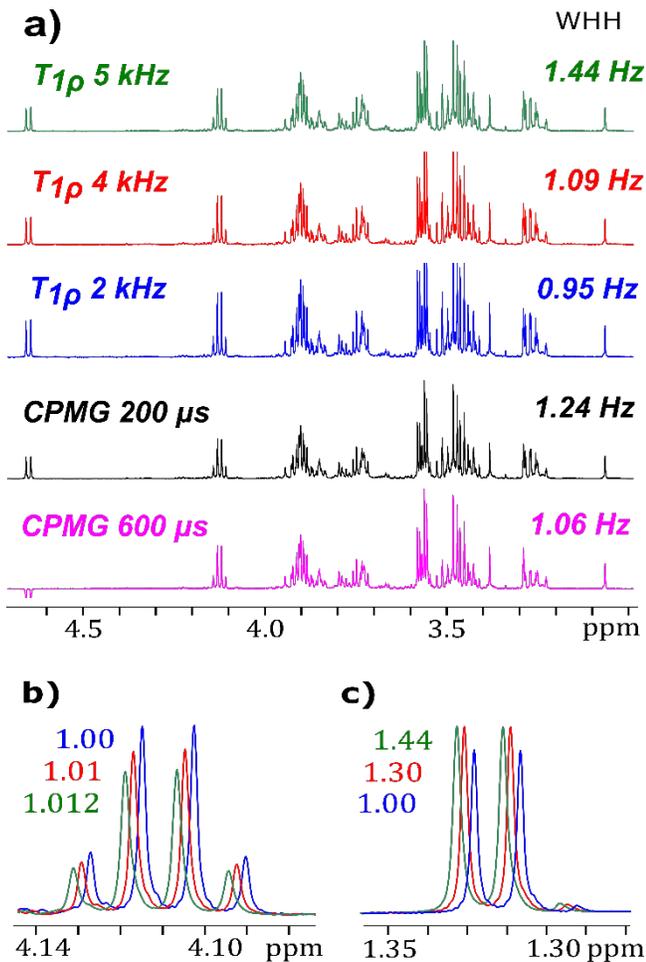
Figure 1. (a) $T_{1\rho}$ and T_2 filtered spectra of serum recorded at different spinlock amplitudes, from top to bottom: 5 kHz, 4 kHz and 2 kHz, and CPMG with inter-pulse delays of 200 and 600 µs. Quartet **(b)** and doublet **(c)** of lactate acquired at 5 kHz (green), 4 kHz (red) and 2 kHz (blue). The relative integrals are reported for each peak with the same colour. The widths at half height (WHH) of the peak at 3.03 ppm (creatine singlet) are reported on the right of each spectrum.

Relaxation time measurement

The measurements of the relaxation times $T_{1\rho}$ and T_2 for some chosen metabolites in serum confirm that these two relaxation rates are substantially similar. **Figure 2** depicts the evolution of the relaxation rates (inverse of the relaxation times) $R_{1\rho}$ as a function of the nutation frequency (ν_1) and R_2 as a function of ν_{CPMG}. The evolution of the R_2 and $R_{1\rho}$ are different. The stability of the R_2 measurements (**Figure 2a and 2c**) depends on: i) signal modulation due to the imperfect refocusing of the J-couplings, ii) the imperfections of π pulses, iii) the various slow molecular dynamics as well as iv) the influence of the ^{1}H carrier during the CPMG block (offset effect). Recently, Heiner N. Raum *et al.*[56] demonstrated that it is possible to obtain an artefact-free relaxation dispersion profile if CPMG pulses are applied on resonant (below 300 Hz). However, R_2 is stable and independent of the ν_{CPMG}, except for creatine. The measurements were limited to $CPMG_{100\mu s}^{2.5\,kHz}$ to prevent sample overheating and possible harmful effect due to too short pulse switching times. We are not able to thoroughly explain the

unusual evolution of creatine R_2 associated with a high relaxation rate. This can be due, for example, to possible intermolecular interactions with exchange effects observed even in liquid state NMR. [57-58].

The stability of the $R_{1\rho}$ measurements (**Figure 2b and 2d**) depends on the slow molecular dynamics and especially on the offset effect. This effects are visible at low spin-lock amplitudes, below $\nu_1 = 2.5$ kHz. More interestingly for the practical aspect, the dispersion curves show that above 3 kHz, the $R_{1\rho}$ stabilizes for most peaks. This results confirm that the previously designated spin-lock amplitude (4 kHz, red circle) is an adequate value for serum samples.
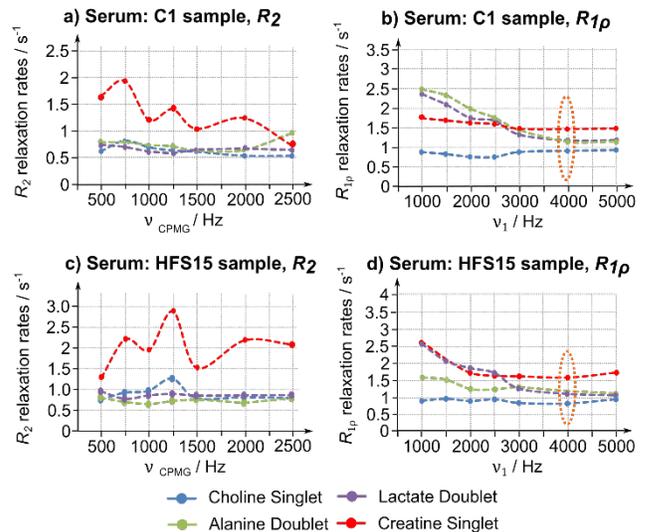

Figure 2. R_2 and $R_{1\rho}$ relaxation rates as a function of ν_{CPMG} and ν_1 respectively for C and HFS serum samples relative to peaks of four metabolites. **(a)** R_2 and **(b)** $R_{1\rho}$ for the C1 sample, **(c)** R_2 and **(d)** $R_{1\rho}$ for the HFS15 sample. Dotted lines are used to help visually track the progress of $R_{1\rho}$.

To assess these differences, the spectra of all the groups (control and HFS groups), labelled as a function of the used sequence, were submitted to statistical analysis. OPLS-DA was performed for the four sequences: $CPMG_{200\mu s}^{1,25kHz}$ (commonly used in metabolomics), $T_{1\rho}^{2kHz}$, $T_{1\rho}^{4kHz}$, $T_{1\rho}^{5kHz}$. The score plot (**Figure 3a**) shows a significant difference between the $T_{1\rho}$ and T_2 weighted spectra. The **Figure 3b** presents the analysis of the $T_{1\rho}$ filtered spectra obtained with different spin-lock amplitudes and shows a clear difference between the $T_{1\rho}^{2kHz}$ and $T_{1\rho}^{4kHz,\,5kHz}$. As mentioned above, this expected difference is the consequence of the offset effect resulting from a non-sufficient spin-lock amplitude to cover the entire spectrum. When comparing $T_{1\rho}^{4kHz}$ and $T_{1\rho}^{5kHz}$ spectra, the score plot (**Figure 3c**) indicates that no statistically significant difference was observed since $\frac{\gamma B_1}{2\pi}$ of 4 kHz is sufficient to cover the overall region containing the signals of interest. A global analysis performed on the spectra shows that it is the intensities of the global spectrum which discriminates the CPMG from the $T_{1\rho}$, whereas it is actually the areas at the ends of the spectra which differentiates the $T_{1\rho}^{2kHz}$ from $T_{1\rho}^{4kHz}$ and $T_{1\rho}^{5kHz}$.
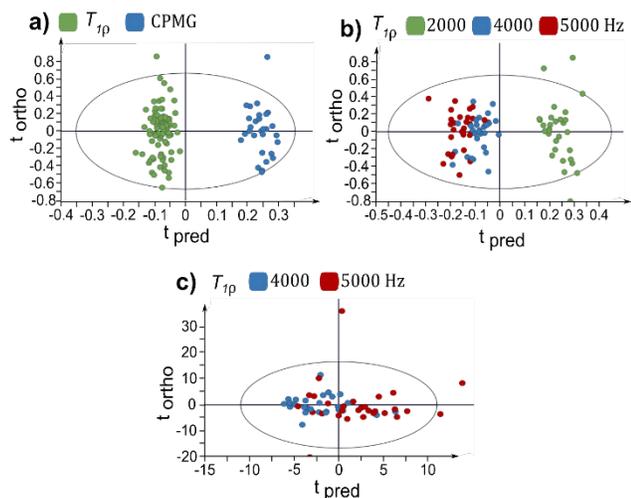
Figure 3. The OPLS-DA score plots of rat serum samples of HFS and C groups with duplicates, **a)** $T_{1\rho}$ vs. CPMG (N=117, R^2_Y=0,965, Q^2_Y=0,903, p-value=1,652x10^{-30}), **b)** data from $T_{1\rho}$ sequences at different spin lock amplitudes: 2kHz (green), 4kHz (blue) and 5kHz (red) (N=88, R^2_Y=0,472, Q^2_Y=0,425, p-value=7,0746x10^{-17}), **c)** $T_{1\rho}$ at 4kHz (blue) vs. 5kHz (red) (N=58, R^2_Y=0,268, Q^2_Y= -0,175, p-value=1).

Effect of B_1 amplitudes on statistical analysis

To compare the separation capability of $T_{1\rho}$ and T_2 filtered spectra, OPLS-DA was performed to discriminate the C and HFS groups. The score plots are presented in **Figure 4**, where, the two OPLS component models (1 predictive + 1 orthogonal component) display a clear discrimination between HFS and control samples with comparable statistical results obtained for all sequences (Table in **SI.5.**). These results show that the properties of each of the experiments used are reproducible and allow discrimination between groups by multivariate analysis. In addition, the loading plots exhibit the same profile for all the sequences with identical correlation coefficients.

The choice of the appropriate experiment may be guided by reviewing the pros and cons of each sequence. The $T_{1\rho}^{4kHz}$ seems to be the best compromise between optimal spectral coverage and the use of moderated spin-lock amplitude. Even if we consider that the amplitude of $T_{1\rho}^{5kHz}$ is not excessive, especially with the filter lengths commonly used in metabolomics (between 60ms and 100ms), knowing that in our study, the filter duration of 480 ms was applied and chosen by eye to eliminate all the broad signals, including those of lipids, to process only the signals of the metabolites, we must point out the only drawback concerning the lower resolution obtained with this amplitude, which remains however safe to use. $T_{1\rho}^{2kHz}$, as seen above, is characterized by a significant offset effect and should be ruled out.
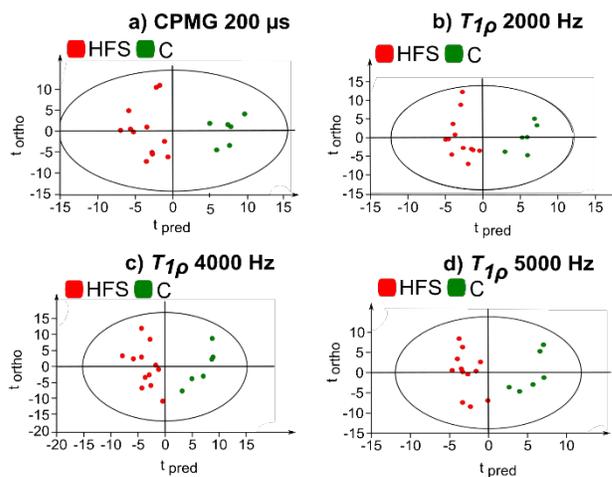

Figure 4. OPLS-DA score plots for N=18 rat serum samples comparing the distribution of the HFS group with the C group using different sequences: **(a)** CPMG 200 μs, **(b)** $T_{1\rho}$: at 2000 Hz, **(c)** $T_{1\rho}$: at 4000 Hz, **(d)**: $T_{1\rho}$ at 5000 Hz.

Assessment of $T_{1\rho}$ filter on HR-MAS metabolomic studies

The relevance of the use of the $T_{1\rho}$ filter for HR-MAS metabolomic studies has never been discussed or considered in the literature. Conventionally, HR-MAS metabolomic studies are carried out by using CPMG filtered spectra at a relatively fast spinning rate (4 kHz). In this case, rotor synchronization does not seem to be a drawback and leads to relatively short inter-pulse delays (250 μs) that can be considered as sufficient to refocus the J-modulation, even if this refocusing is imperfect. For HR-MAS experiments at low spinning rates (1 kHz, for example), rotor synchronization leads to a long inter-pulse delay (1 ms) and the PROJECT sequence is therefore preferred to successfully generate spectra without "J-modulation artifacts". $T_{1\rho}$ filtered experiment can be a simple and efficient alternative since there is no precession during the evolution period of the magnetization and therefore no J-modulation artifacts. However, some properties related to the dependence of $T_{1\rho}$ to the nutation (ν_1) and the rotation (ν_r) frequencies, in addition to the obvious contribution of slow dynamic processes have to be taken into account. To our knowledge, no data report the behaviour of the $T_{1\rho}$ of metabolites measured in tissues by HR-MAS. On the other hand, several applications are using $T_{1\rho}$ for the determination of the local dynamics of proteins by MAS.[59-61] In this field, a comprehensive article that addresses these aspects on slow motions in microcrystalline proteins by MAS was recently published by Krushelnitsky *et al.*[62]. The authors presented the MAS dependence of the relaxation rate $R_{1\rho}$, which was modulated by correlation times of slow motions (from 10 μs to 1 ms). In semi-solid samples, one can expect a contribution of both isotropic and anisotropic interaction to the relaxation mechanisms.[63] In order to know the behaviour of $T_{1\rho}$ experiments, we measured the $R_{1\rho}$ at the two spinning rates, 1000 Hz and 4000 Hz, commonly used in HR-MAS metabolomics, and for selected B_1 amplitude values.

In HR-MAS studies of tissues, the possible degradation of the samples is an important issue. Indeed, at a relatively high spinning rate (4 kHz, for example), tissue degradation can lead to the release of metabolites into the extracellular medium, resulting in narrowing peaks over the experiments and therefore bias the comparison. Recently, the impact of freezing and prolonged HR-MAS Analysis on the metabolic profile shows

that after 1.5h with a spinning rate of 5000Hz, the levels of certain metabolites change.[64] In this study, the total experiment time, for the 6 experiments (two MAS rates), was about 1 hour (10 min per experiment, CPMG / PROJECT / $T_{1\rho}$), starting with the slow spinning rate (1000 Hz). The relaxation measurement depicted in Figure 5 was done on freshly prepared samples from pieces of liver stored at -80°C, with a total experiment time of about 2 hours, during which we did not observe significant changes in the spectra even after two hours. Moreover, tissue degradation during the NMR experiments was avoided by maintaining the sample at 4°C.

We report in **Figure 5** the relaxation rates $R_{1\rho}\left(=\frac{1}{T_{1\rho}}\right)$ of some selected metabolites for one randomly chosen sample (Control-3) to assess its evolution as a function of B_1 expressed by the nutation frequency $\left(\upsilon_1 = \frac{\gamma B_1}{2\pi}\right)$ for the two MAS spinning rates, 1000Hz (**Figure 5a**) and 4000Hz (**Figure 5b**).

Creatine Singlet
Choline Singlet
Lactate Doublet
β-D-Glucose Doublet
Glycerophosphocholine Singlet
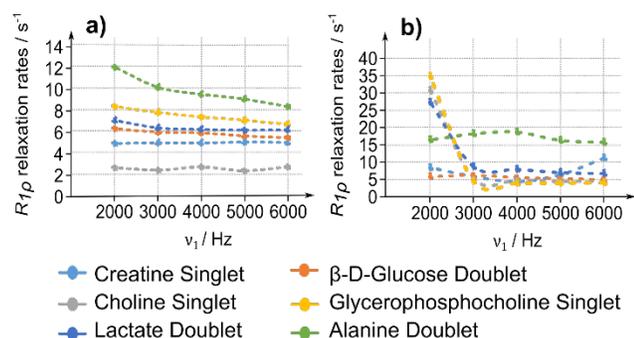Alanine Doublet

Figure 5. $R_{1\rho}$ as a function of υ_1 for liver control sample (C3) relative to six different peaks of six metabolites **(a)** at $\nu_r = 1000$ Hz and **(b)** at $\nu_r = 4000$ Hz. Dotted lines are used to help visually track the progress of $R_{1\rho}$.

The general observation concerns the MAS dependence of the relaxation rates, which confirms the behaviour reported in the literature in the solid state.[62] If we focus on $\upsilon_1 = 4000$Hz, which was defined as optimal in the liquid study (as a better compromise for a moderated amplitude, sufficient spectral coverage, and better resolution), one can analyse quantitatively these evolutions (**Table SI.6.**). For certain metabolites, probably depending on the slow dynamic contribution, $R_{1\rho}$ increases with the MAS spinning rate (lactate doublet and glycerophosphocholine singlet, for example), for others, its remains substantially the same (creatine singlet and β-D-glucose doublet), and for some others, it decreases (i.e., choline singlet). These expected results, due to the heterogeneity of the tissues analyzed in HR-MAS, do not constitute a drawback for metabolomic applications since the behaviour of each metabolite is reproducible through different samples. However, the stability of the relaxation values around the chosen υ_1 (4000 Hz) is critical. For both MAS spinning rates, we found that around this value the relaxation rates would not be drastically affected by the expected slight variation of B_1 due to eventual different probe tuning from sample to sample.

To assess qualitatively the reproducibility, we recorded the T_2- and $T_{1\rho}$-edited spectra for three samples taken from the same control liver (**SI.7.**). The $T_{1\rho}$ and PROJECT filtered spectra are identical whatever the MAS spinning rate ($\nu_r = 1000$Hz and 4000Hz), while the CPMG filtered spectra present at $\nu_r =$

1000Hz J-artefacts which result in negative signals and an intensity loss, especially between 1.5 - 3 ppm.

Statistical analysis
The spectra obtained with each pulse sequence (CPMG, PROJECT and $T_{1\rho}$) have the same filtration effect but the profiles show predictable intensity differences due to the different mechanisms involved in each relaxation filter.[65] The impact of these differences on the statistical processing obviously depends on the reproducibility of the artefacts of each sequence and on the modulations (due to exchange phenomena, for example) resulting from the adaptation of the inter-pulse delays to the rotation frequency ν_r. Another important experimental consideration is to avoid the synchronization of the spinning frequency ν_r with the spin-lock frequency ν_1. Indeed, this leads to a recoupling of the CSA, dipolar interactions, and magnetic susceptibility effects, which results in a loss of resolution.[66-67] To avoid these contributions, we used a spin-lock amplitude of 4.3 kHz for both used spinning rates (4 kHz and 1 kHz). **Figure SI.8.a** presents an OPLS-DA of all spectra obtained with a rotation rate of 4 kHz. It shows that CPMG and PROJECT spectra are relatively similar and significantly different from the $T_{1\rho}$ filtered one. Interestingly, at low spinning rate (1 kHz), **Figure SI.8.b,** the synchronization of the inter-pulse delays (1 ms) leads to a significant discrimination between CPMG and PROJECT filtered spectra due to the J modulation effect, which is not compensated with the CPMG sequence. These differences can be assessed in a relevant way, directly on the spectra, however, statistical tools allow to evaluate the overall "inter-sequence" differences and the "intra-sequence" reproducibility.

The OPLS-DA multivariate analysis on the two groups (Control vs. HFS) that enables to evaluate the separation capability and the steadiness of $T_{1\rho}$ and T_2 filtered spectra obtained at the two spinning rates, 1 kHz and 4 kHz are depicted in **Figure 7** and **Figure 8**, respectively. Whatever the spinning rate, the main observation is that the discrimination between the two groups is clear and the score plots obtained with the $T_{1\rho}$ filter (**Figure 7 and 8**) provide similar statistical parameters to those obtained with PROJECT and CPMG (Table **SI.9.**).

The intragroup variation for the HFS group observed whatever the experiment, can be explained by taking into account the inhomogeneity of response of complex organisms to an external imbalance[68-69] (here a food imbalance). This effect is observed on several parameters (overall weight of animals, gain weight, normalized liver weights, HOMA-IR levels, serum glucose, triglycerides, cholesterol and insulin levels). In the previous article which dealt with these samples,[44] we clearly noted an increase of the standard deviation for all these parameters when we pass from controls to an increasing introduction of the number of external stimuli or imbalance (standard diet, HFS diet, HFS diet plus medication), see **SI.10.** Conversely, this dispersion is usually lower or even absent for the control groups.[44] However, whatever the sequence used, this intra-group reproducibility is not found at $\nu_r = 1$ kHz (Figure **SI.11.**) because of the non-reproducible sidebands present in the spectra, depending on sample preparation. At $\nu_r = 4$ kHz, the absence of the sidebands allows to retrieve the intra-group reproducibility for the control group (**Figure 6**).
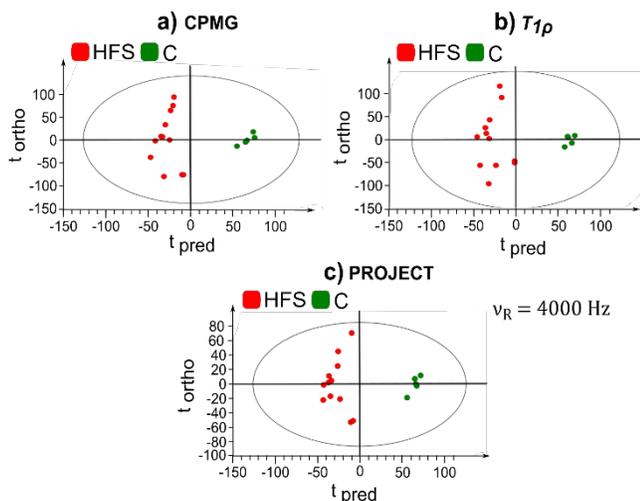
Figure 6. Multivariate analysis using OPLS-DA performed on liver samples for the two groups: C and HFS obtained for each sequence: CPMG (a), $T_{1\rho}$ (b) and PROJECT (c), at v_r =4 kHz.

These results show that the artefacts inherent in each sequence are reproducibly replicated over the samples and multivariate analysis allows discrimination between the groups, including the CPMG sequence at $v_r = 1000$Hz which present J-artefacts (negative signals and an intensity loss especially between 1.5-3 ppm) due to the long inter-pulse delay (1ms) used for rotor synchronization (**SI.7.**). However, this sequence must obviously be excluded since the quality of the spectra does not allow an accurate determination of the discriminant spectral regions. The $T_{1\rho}$ and PROJECT filtered spectra are identical for the two MAS spinning rates ($v_r = 1000$Hz and 4000Hz) and the loading plots provide the same profiles with comparable correlation coefficients (**SI.13.** and **SI.14.**).

Conclusions

In this article, we have shown the application of the $T_{1\rho}$ filter in metabolomics on liquid samples and on tissues by HR-MAS. It is characterized by the absence of modulations due to scalar couplings, its simple implementation that needs no calculation for adjusting the duration of the filters, and no synchronization is required whatever the HR-MAS spinning rate. Despite these proven advantages, its generalization does not yet seem obvious and remains "rejected", probably by the fear of overheating that would be caused by the spin-locking. For the filter duration (hundreds of milliseconds) and also the powers used in metabolomics (up to 5 kHz), the heating is not a drawback. It is important to note that the work presented in this article relates to spectrometers operating at 400 MHz and 600 MHz. If metabolomic experiments with a $T_{1\rho}$ filter were to be carried out with higher magnetic field, 800 MHz for example, the power of the spin-lock may not be sufficient to cover the entire spectrum. To avoid the offset effects, it will be necessary to use higher powers (6 KHz or 7 kHz), that, taking into account the metabolomic duration of the filters, will have no deleterious effect. Moreover, we showed that if moderated offset effect is present, the analysis of the results leads to the same observations: the inter-group discrimination, and the extraction of the discriminant spectral regions from the loading plots. However, the developments and the implementation of the offset methods used in solid state NMR[70] to enhance the total effective field of the spin-lock represent an interesting prospect

for wider spectral covers in metabolomics. Further developments and adaptations to the metabolomics with an evaluation of the impacts on statistical analyses will be expected in the future. As it was presented in the introduction, it is important to reduce the amount of pre-treatment steps to handle the samples as little as possible to avoid introducing errors. We can transpose this reflection to the relaxation filters, the CPMG consists in manipulating the magnetization by π pulse train, allowing the precession and introducing "artificially" modulations because of the scalar couplings that do not seem to be completely refocused. With the $T_{1\rho}$ filter, magnetization is "less handled", it is locked on a transverse axis (hence no precession) during a time during which the signals of the macromolecules disappear. Thus, the sequence that introduces the least artefact would be most suitable for fields where the quantitative aspect is very important as in metabolomics. Consideration of the $T_{1\rho}$ filter in metabolomics would undoubtedly lead to developments for the implementation of different spin-lock schemes, and the reduction of the powers used while eliminating/minimizing the offset effects.

ASSOCIATED CONTENT

Supporting Information
A listing of the contents supplied as Supporting Information is included.
Table **SI.1.** Number of independent samples in each analyzed group. Figure **SI.2.** Pulse program and implementation. Table **SI.3**. Temperatures measured from ^{1}H spectra of methanol-d4 using one pulse (zg), CPMG and $T_{1\rho}$ sequences with the same delay of 480 ms, different number of dummy scans (DS) were used, with number of scans NS=1. Target sample temperature was set to 277 K. The actual T was calculated by TopSpin "calctemp" command. The difference between the target and actual temperature is reported. Table **SI.4**. Width at half height of the creatine singlet (3.03 ppm) [Average over five randomly selected samples]. Table **SI.5.** The OPLS-DA R^2_Y, Q^2_Y and p-values for HFS vs. C serum samples. Table **SI.6.** $R_{1\rho}$ evolution of some chosen metabolites, from liver sample C3, as a function of spinning (v_R) and nutation (v_1) frequency. Figure **SI.7.** T_2- and $T_{1\rho}$-edited spectra for three samples taken from the same control liver, sample C2. (A) CPMG, (B) T1ρ, (C) PROJECT. In red the spectra acquired at $v_R = 4000$ Hz, in blue at $v_R = 1000$ Hz. Table **SI.8.** The OPLS-DA R^2_Y, Q^2_Y and p-values for HFS vs. C samples of livers without one outlier (with N = number of the samples and A = number of components to fit the model) using UV scaling. Table **SI.9.** Results of serum biochemical analysis and body weight after 10 weeks of diet. Figure **SI.10.** Multivariate analysis using OPLS-DA performed on liver samples for the two groups: C and HFS obtained for each sequence: CPMG (a), $T_{1\rho}$ (b) and PROJECT (c), at v_r =1 kHz. Figure **SI.11.** Multivariate analysis using OPLS-DA performed on liver samples for the two groups: C and HFS obtained for each sequence: CPMG (a), $T_{1\rho}$ (b) and PROJECT (c), at v_r =4 kHz. Figure **SI.12.** S-line plots of the OPLS-DA models of Figure SI.10. for CPMG, T$_{1\rho}$, PROJECT at $v_R = 1000$ Hz for liver samples. Figure **SI.13.** S-line plots of the OPLS-DA models of Figure SI.11. for CPMG, $T_{1\rho}$, PROJECT at $v_R= 4000$ Hz for liver samples.

The Supporting Information is available free of charge on the ACS Publications website.

AUTHOR INFORMATION

Corresponding Author

*Mehdi Yemloul - Department of Chemistry, Aix-Marseille Université, Marseille, France ; *E-mail: mehdi.yemloul@univ-amu.fr .

Notes

The authors declare no competing financial interest.

Author Contributions

The manuscript was written through contributions of all authors. All authors have given approval to the final version of the manuscript.

REFERENCES

1. Jobard, E.; Tredan, O.; Postoly, D.; Andre, F.; Martin, A. L.; Elena-Herrmann, B.; Boyault, S., A Systematic Evaluation of Blood Serum and Plasma Pre-Analytics for Metabolomics Cohort Studies. *Int J Mol Sci* **2016,** *17* (12).

2. Suarez-Diez, M.; Adam, J.; Adamski, J.; Chasapi, S. A.; Luchinat, C.; Peters, A.; Prehn, C.; Santucci, C.; Spyridonidis, A.; Spyroulias, G. A.; Tenori, L.; Wang-Sattler, R.; Saccenti, E., Plasma and Serum Metabolite Association Networks: Comparability within and between Studies Using NMR and MS Profiling. *J Proteome Res* **2017,** *16* (7), 2547-2559.

3. Carr, H. Y.; Purcell, E. M., Effects of Diffusion on Free Precession in Nuclear Magnetic Resonance Experiments. *Physical Review* **1954,** *94* (3), 630-638.

4. Andre, M.; Dumez, J. N.; Rezig, L.; Shintu, L.; Piotto, M.; Cadarelli, S., Complete Protocol for Slow-Spinning High-Resolution Magic-Angle Spinning NMR Analysis of Fragile Tissues. *Anal. Chem.* **2014,** *86* (21), 10749-10754.

5. Weininger, U.; Respondek, M.; Low, C.; Akke, M., Slow Aromatic Ring Flips Detected Despite Near-Degenerate NMR Frequencies of the Exchanging Nuclei. *J Phys Chem B* **2013,** *117* (31), 9241-9247.

6. Meiboom, S.; Gill, D., Modified Spin-Echo Method for Measuring Nuclear Relaxation Times. *Review of Scientific Instruments* **1958,** *29* (8), 688-691.

7. Mahi, L.; Duplan, J. C.; Fenet, B., Suppression of J-Modulation Effects for Resonance Editing by Nmr Spin-Echo Experiments. *Chemical Physics Letters* **1993,** *211* (1), 27-30.

8. Weitekamp, D. P.; Garbow, J. R.; Pines, A., Determination of Dipole Coupling-Constants Using Heteronuclear Multiple Quantum Nmr. *J Chem Phys* **1982,** *77* (6), 2870-2883.

9. Botana, A.; Aguilar, J. A.; Nilsson, M.; Morris, G. A., J-modulation effects in DOSY experiments and their suppression: The Oneshot45 experiment. *J Magn Reson* **2011,** *208* (2), 270-278.

10. Pell, A. J.; Keeler, J., Two-dimensional J-spectra with absorption-mode lineshapes. *J Magn Reson* **2007,** *189* (2), 293-299.

11. Mandelshtam, V. A.; Van, Q. N.; Shaka, A. J., Obtaining proton chemical shifts and multiplets from several 1D NMR signals. *J Am Chem Soc* **1998,** *120* (46), 12161-12162.

12. Barrere, C.; Thureau, P.; Thevand, A.; Viel, S., A convenient method for the measurements of transverse relaxation rates in homonuclear scalar coupled spin systems. *Chem. Commun.* **2011,** *47* (32), 9209-9211.

13. Aguilar, J. A.; Nilsson, M.; Bodenhausen, G.; Morris, G. A., Spin echo NMR spectra without J modulation. *Chem. Commun.* **2012,** *48* (6), 811-813.

14. Takegoshi, K.; Ogura, K.; Hikichi, K., A Perfect Spin-Echo in a Weakly Homonuclear J-Coupled 2 Spin-1/2 System. *J Magn Reson* **1989,** *84* (3), 611-615.

15. Vanzijl, P. C. M.; Moonen, C. T. W.; Vonkienlin, M., Homonuclear-J Refocusing in Echo Spectroscopy. *J Magn Reson* **1990,** *89* (1), 28-40.

16. Torres, A. M.; Zheng, G.; Price, W. S., J-compensated PGSE: an improved NMR diffusion experiment with fewer phase distortions. *Magn. Reson. Chem.* **2010,** *48* (2), 129-133.

17. Tollinger, M.; Sivertsen, A. C.; Meier, B. H.; Ernst, M.; Schanda, P., Site-Resolved Measurement of Microsecond-to-Millisecond Conformational-Exchange Processes in Proteins by Solid-State NMR Spectroscopy. *J Am Chem Soc* **2012,** *134* (36), 14800-14807.

18. Redfied, A. G. Nuclear Magnetic Resonance Saturation and Rotary Saturation in Solids. *Physical Review* **1955**, 1787(98), 1787-1809.

19. Novoa-Carballal, R.; Fernandez-Megia, E.; Jimenez, C.; Riguera, R., NMR methods for unravelling the spectra of complex mixtures. *Nat. Prod. Rep.* **2011,** *28* (1), 78-98.

20. Quinn, C. M.; McDermott, A. E., Quantifying conformational dynamics using solid-state R-1 rho experiments. *J Magn Reson* **2012,** *222*, 1-7.

21. Sepponen, R. E.; Pohjonen, J. A.; Sipponen, J. T.; Tanttu, J. I., A Method for T1-Rho Imaging. *Journal of Computer Assisted Tomography* **1985,** *9* (6), 1007-1011.

22. Gonyea, J. V.; Watts, R.; Applebee, A.; Andrews, T.; Hipko, S.; Nickerson, J. P.; Thornton, L.; Filippi, C. G., In Vivo Quantitative Whole-Brain T-1 rho MRI of Multiple Sclerosis. *J. Magn. Reson. Imaging* **2015,** *42* (6), 1623-1630.

23. Wang, Y. X. J.; Zhao, F.; Griffith, J. F.; Mok, G. S. P.; Leung, J. C. S.; Ahuja, A. T.; Yuan, J., T1rho and T2 relaxation times for lumbar disc degeneration: an in vivo comparative study at 3.0-Tesla MRI. *Eur Radiol* **2013,** *23* (1), 228-234.

24. Andronesi, O. C.; Bhat, H.; Reuter, M.; Mukherjee, S.; Caravan, P.; Rosen, B. R., Whole brain mapping of water pools and molecular dynamics with rotating frame MR relaxation using gradient modulated low-power adiabatic pulses. *Neuroimage* **2014,** *89*, 92-109.

25. Paul, C. P. L.; Smit, T. H.; de Graaf, M.; Holewijn, R. M.; Bisschop, A.; van de Ven, P. M.; Mullender, M. G.; Helder, M. N.; Strijkers, G. J., Quantitative MRI in early intervertebral disc degeneration: T1 rho correlates better than T2 and ADC with biomechanics, histology and matrix content. *Plos One* **2018,** *13* (1).

26.   Solomon, I., Rotary Spin Echoes. *Phys. Rev. Lett.* **1959,** *2* (7), 301-302.

27.   Mangia, S.; Liimatainen, T.; Garwood, M.; Michaeli, S., Rotating frame relaxation during adiabatic pulses vs. conventional spin lock: simulations and experimental results at 4 T. *Magn Reson Imaging* **2009,** *27* (8), 1074-1087.

28.   Chen, W., Errors in quantitative T1rho imaging and the correction methods. *Quant Imaging Med Su* **2015,** *5* (4), 583-591.

29.   Witschey, W. R. T.; Borthakur, A.; Elliott, M. A.; Mellon, E.; Niyogi, S.; Wang, C. Y.; Reddy, R., Compensation for spin-lock artifacts using an off-resonance rotary echo in T-1 rho(off)-weighted imaging. *Magn Reson Med* **2007,** *57* (1), 2-7.

30.   Wheaton, A. J.; Casey, F. L.; Gougoutas, A. J.; Dodge, G. R.; Borthakur, A.; Lonner, J. H.; Schumacher, H. R.; Reddy, R., Correlation of T-1 rho with fixed charge density in cartilage. *J. Magn. Reson. Imaging* **2004,** *20* (3), 519-525.

31.   Scherf, T.; Anglister, J., A T1 rho-filtered two-dimensional transferred NOE spectrum for studying antibody interactions with peptide antigens. *Biophys J* **1993,** *64* (3), 754-61.

32.   Grelard, A.; Loudet, C.; Diller, A.; Dufourc, E. J., NMR Spectroscopy of Lipid Bilayers. *Methods Mol Biol* **2010,** *654,* 341-359.

33.   Puthenveetil, R.; Nguyen, K.; Vinogradova, O., Nanodiscs and solution NMR: preparation, application and challenges. *Nanotechnol Rev* **2017,** *6* (1), 111-125.

34.   Opella, S. J.; Marassi, F. M., Applications of NMR to membrane proteins. *Arch Biochem Biophys* **2017,** *628,* 92-101.

35.   Sanders, C. R.; Prosser, R. S., Bicelles: a model membrane system for all seasons? *Struct Fold Des* **1998,** *6* (10), 1227-1234.

36.   Lind, J.; Nordin, J.; Maler, L., Lipid dynamics in fast-tumbling bicelles with varying bilayer thickness: Effect of model transmembrane peptides. *Bba-Biomembranes* **2008,** *1778* (11), 2526-2534.

37.   Bodor, A.; Kover, K. E.; Maler, L., Membrane interactions in small fast-tumbling bicelles as studied by 31P NMR. *Biochim Biophys Acta* **2015,** *1848* (3), 760-6.

38.   Awosanya, E. O.; Nevzorov, A. A., Protein Rotational Dynamics in Aligned Lipid Membranes Probed by Anisotropic T-1 rho NMR Relaxation. *Biophysical Journal* **2018,** *114* (2), 392-399.

39.   Durr, U. H.; Yamamoto, K.; Im, S. C.; Waskell, L.; Ramamoorthy, A., Solid-state NMR reveals structural and dynamical properties of a membrane-anchored electron-carrier protein, cytochrome b5. *J Am Chem Soc* **2007,** *129* (21), 6670-1.

40.   Xu, J. D.; Zhu, P. Z.; Morris, M. D.; Ramamoorthy, A., Solid-State NMR Spectroscopy Provides Atomic-Level Insights Into the Dehydration of Cartilage. *J Phys Chem B* **2011,** *115* (33), 9948-9954.

41.   Li, X. J.; Cheng, J. N.; Lin, K. R.; Saadat, E.; Bolbos, R. I.; Jobke, B.; Ries, M. D.; Horvai, A.; Link, T. M.; Majumdar, S., Quantitative MRI using T-1 rho, and T-2 in human osteoarthritic cartilage specimens: correlation with biochemical measurements and histology. *Magn Reson Imaging* **2011,** *29* (3), 324-334.

42.   Tang, H. R.; Wang, Y. L.; Nicholson, J. K.; Lindon, J. C., Use of relaxation-edited one-dimensional and two dimensional nuclear magnetic resonance spectroscopy to improve detection of small metabolites in blood plasma. *Analytical Biochemistry* **2004,** *325* (2), 260-272.

43.   Tranchida, F.; Shintu, L.; Rakotoniaina, Z.; Tchiakpe, L.; Deyris, V.; Hiol, A.; Caldarelli, S., Metabolomic and Lipidomic Analysis of Serum Samples following Curcuma longa Extract Supplementation in High-Fructose and Saturated Fat Fed Rats. *Plos One* **2015,** *10* (8).

44.   Tranchida, F.; Rakotoniaina, Z.; Shintu, L.; Tchiakpe, L.; Deyris, V.; Yemloul, M.; Stocker, P.; Vidal, N.; Rimet, O.; Hiol, A.; Caldarelli, S., Hepatic metabolic effects of Curcuma longa extract supplement in high-fructose and saturated fat fed rats. *Sci Rep* **2017,** *7.*

45.   Beckonert, O.; Keun, H. C.; Ebbels, T. M.; Bundy, J.; Holmes, E.; Lindon, J. C.; Nicholson, J. K., Metabolic profiling, metabolomic and metabonomic procedures for NMR spectroscopy of urine, plasma, serum and tissue extracts. *Nat Protoc* **2007,** *2* (11), 2692-703.

46.   Trygg, J.; Wold, S., Orthogonal projections to latent structures (O-PLS). *J. Chemometrics* **2002,** *16* (3), 119-128.

47.   Wishart, D. S., Current Progress in computational metabolomics. *Briefings in Bioinformatics* **2007,** *8* (5), 279-293.

48.   Westerhuis, J. A.; Hoefsloot, H. C. J.; Smit, S.; Vis, D. J.; Smilde, A. K.; van Velzen, E. J. J.; van Duijnhoven, J. P. M.; van Dorsten, F. A., Assessment of PLSDA cross validation. *Metabolomics* **2008,** *4* (1), 81-89.

49.   Worley, B.; Powers, R., Multivariate Analysis in Metabolomics. *Curr Metabolomics* **2013,** *1* (1), 92-107.

50.   Yip, G. N. B.; Zuiderweg, E. R. P., Improvement of duty-cycle heating compensation in NMR spin relaxation experiments. *J Magn Reson* **2005,** *176* (2), 171-178.

51.   Ban, D.; Gossert, A. D.; Giller, K.; Becker, S.; Griesinger, C.; Lee, D., Exceeding the limit of dynamics studies on biomolecules using high spin-lock field strengths with a cryogenically cooled probehead. *J Magn Reson* **2012,** *221,* 1-4.

52.   Khoshnood, A.; Lukanov, B.; Firoozabadi, A., Temperature Effect on Micelle Formation: Molecular Thermodynamic Model Revisited. *Langmuir* **2016,** *32* (9), 2175-2183.

53.   Oremusova, J.; Vitkova, Z.; Vitko, A.; Tarnik, M.; Miklovicova, E.; Ivankova, O.; Murgas, J.; Krchnak, D., Effect of Molecular Composition of Head Group and Temperature on Micellar Properties of Ionic Surfactants with C12 Alkyl Chain. *Molecules* **2019,** *24* (3).

54.   Yamamoto, K.; Gildenberg, M.; Ahuja, S.; Im, S. C.; Pearcy, P.; Waskell, L.; Ramamoorthy, A., Probing the Transmembrane Structure and Topology of Microsomal Cytochrome-P450 by Solid-State NMR on Temperature-Resistant Bicelles. *Sci Rep* **2013,** *3.*

55.   Holly, R.; Peemoeller, H.; Choi, C.; Pintar, M. M., Proton rotating frame spin-lattice relaxation study of slow motion of pore water. *J Chem Phys* **1998,** *108* (10), 4183-4188.

56.   Raum, H. N.; Dreydoppel, M.; Weininger, U., Conformational exchange of aromatic side chains by H-1 CPMG relaxation dispersion. *J Biomol NMR* **2018,** *72* (1-2), 105-114.

57.   Yemloul, M.; Adyatmika, I. M.; Caldarelli, S.; Ollivier, D.; Campredon, M., Rapid characterization of cocaine in illicit drug samples by 1D and 2D NMR spectroscopy. *Anal Bioanal Chem* **2018,** *410* (21), 5237-5244.

58.   Takis, P. G.; Schafer, H.; Spraul, M.; Luchinat, C., Deconvoluting interrelationships between concentrations and

chemical shifts in urine provides a powerful analysis tool. *Nat Commun* **2017,** *8*.

59.   Lewandowski, J. R.; Sass, H. J.; Grzesiek, S.; Blackledge, M.; Emsley, L., Site-Specific Measurement of Slow Motions in Proteins. *J Am Chem Soc* **2011,** *133* (42), 16762-16765.

60.   Ma, P. X.; Haller, J. D.; Zajakala, J.; Macek, P.; Sivertsen, A. C.; Willbold, D.; Boisbouvier, J.; Schanda, P., Probing Transient Conformational States of Proteins by Solid-State R11 Relaxation- Dispersion NMR Spectroscopy. *Angew Chem Int Edit* **2014,** *53* (17), 4312-4317.

61.   Yamaguchi, M.; Tsutsumi, A., Side-Chain Dynamics in Poly(Gamma-Benzyl L-Glutamate) as Studied by High-Resolution Solid-State C-13 Nuclear Magnetic-Relaxation in Rotating Frame. *Polym J* **1993,** *25* (2), 131-139.

62.   Krushelnitsky, A.; Zinkevich, T.; Reif, B.; Saalwachter, K., Slow motions in microcrystalline proteins as observed by MAS-dependent N-15 rotating-frame NMR relaxation. *J Magn Reson* **2014,** *248*, 8-12.

63.   Kurbanov, R.; Zinkevich, T.; Krushelnitsky, A., The nuclear magnetic resonance relaxation data analysis in solids: General R-1/R-1 rho equations and the model-free approach. *J Chem Phys* **2011,** *135* (18).

64.   Haukaas, T. H.; Moestue, S. A.; Vettukattil, R.; Sitter, B.; Lamichhane, S.; Segura, R.; Giskeodegard, G. F.; Bathen, T. F., Impact of Freezing Delay Time on Tissue Samples for Metabolomic Studies. *Front Oncol* **2016,** *6*.

65.   Steiner, E.; Yemloul, M.; Guendouz, L.; Leclerc, S.; Robert, A.; Canet, D., NMR relaxometry: Spin lattice relaxation times in the laboratory frame versus spin lattice relaxation times in the rotating frame. *Chemical Physics Letters* **2010,** *495* (4-6), 287-291.

66.   Gan, Z. H.; Grant, D. M., Rotational Resonance in a Spin-Lock Field for Solid-State Nmr. *Chemical Physics Letters* **1990,** *168* (3-4), 304-308.

67.   Gan, Z. H.; Grant, D. M.; Ernst, R. R., NMR chemical shift anisotropy measurements by RF driven rotary resonance. *Chemical Physics Letters* **1996,** *254* (5-6), 349-357.

68.   Stark, A. H.; Timar, B.; Madar, Z., Adaptation of Sprague Dawley rats to long-term feeding of high fat or high fructose diets. *European Journal of Nutrition* **2000,** *39* (5), 229-234.

69.   Gayles, E. C.; Pagliassotti, M. J.; Prach, P. A.; Koppenhafer, T. A.; Hill, J. O., Contribution of energy intake and tissue enzymatic profile to body weight gain in high-fat-fed rats. *American Journal of Physiology-Regulatory Integrative and Comparative Physiology* **1997,** *272* (1), R188-R194.

70.   Shekar, S. C.; Lee, D. K.; Ramamoorthy, A., Chemical shift anisotropy and offset effects in cross polarization solid-state NMR spectroscopy. *J Magn Reson* **2002,** *157* (2), 223-234.

Evaluation of the rotating-frame relaxation ($T_{1}\rho$) filter and its application in metabolomics as an alternative to the transverse (T_2) relaxation filter

Elena Piersanti[iD], Lamya Rezig, Fabrice Tranchida, Wael El-Houri, Seidou M. Abagana, Mylène Campredon, Laetitia Shintu[iD] and Mehdi Yemloul[iD]*.

Aix Marseille Univ, CNRS, Centrale Marseille, iSm2, Marseille, France.

*Corresponding Author

Dr. Mehdi Yemloul - Department of Chemistry.

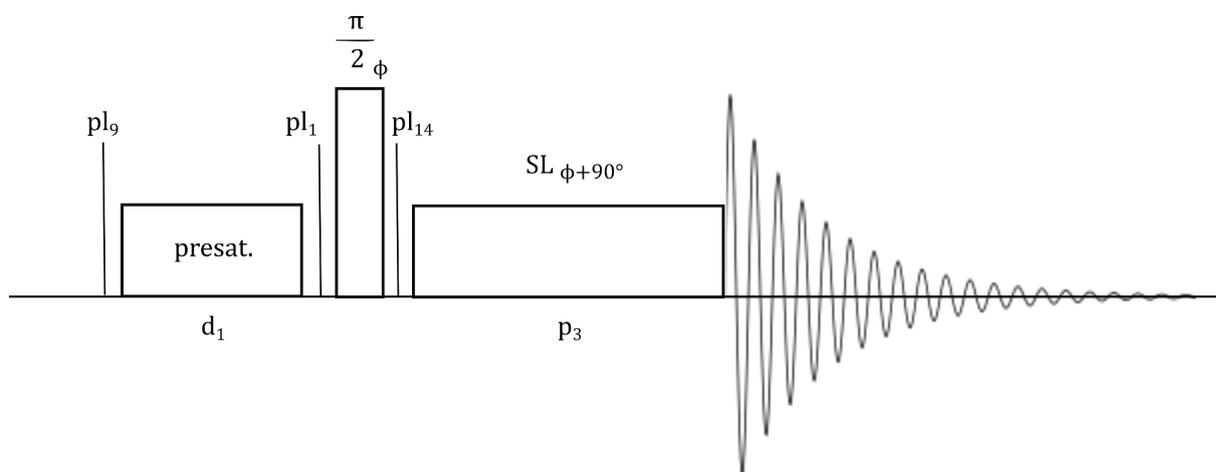Aix-Marseille Université, Marseille, France.

E-mail: mehdi.yemloul@univ-amu.fr .

Table of Contents

Table SI.1. Number of independent samples in each analyzed group.

	Control group	HFS group
Serum	6	12
Liver	6	12

Figure SI.2. Pulse program and implementation

Parameter P3, that concerns the spin-lock length, must be generally set at 100ms and it can be adjusted for more filtration depending on the type of sample.

BRUKER pulse program for 1H pre-saturated $T_{1\rho}$ filtered experiment

```
; avance-version
; 1D sequence

#include <Avance.incl>
#include <Delay.incl>

"p2=p1*2"
"d12=20u"

1 ze
2 30m
  d12 pl9:f1
  d1 cw:f1 ph29
  4u do:f1
  d12 pl1:f1
  p1 ph1
  (p3 pl14 ph10):f1
  go=2 ph31
  30m mc #0 to 2 F0(zd)
```

exit

ph1=0 0 2 2 1 1 3 3
ph10=1 3 1 3 0 2 0 2
ph29=0
ph31=0 0 2 2 1 1 3 3

;pl1 : f1 channel - power level for pulse (default)
;pl14 : f1 channel - power level for spin-lock
;p1 : f1 channel - 90 degree excitation pulse
;p3 : f1 channel – spin-lock duration
;d1 : relaxation delay; 1-5 * T1
;ns: multiples of 4

1 – Calculation of power level for the desired $v_1 = \frac{\gamma B_1}{2\pi}$

a. Calibrate the hard pulse p1.

b. Use the command **"pulse"** in the line command.

c. Enter the desired v_1 (4000Hz or 5000 Hz, for example)

➔ Topspin will return the power level to be used as Plw (watts) and **pl (dB)**.

d. Enter this value in the power level **pl14**

2 – Filter duration:

Enter the filter duration directly on p3 pulse (i.e., use p3 on the line command and enter the suitable duration).**!!! Pay attention to the default unit (μs) !!!**

Table SI.3. Temperatures measured from ^{1}H spectra of methanol-d4 using one pulse (zg), CPMG and $T_{1\rho}$ sequences with the same filter duration (480 ms), different number of dummy scans (DS) were used, with number of scans NS=1. Target sample temperature was set to 277 K. The actual T was calculated by TopSpin "calctemp" command. The difference between the target and actual temperature is reported.

Sequence used	Number of dummy scans	Spin-lock amplitude (Hz)	Δ Temperature (K)
zg			=0
CPMG			+0.10
	1	2000	+0.16
T1ρ		4000	+0.12
		5000	+0.15
zg			=0
CPMG			+0.10
	7	2000	+0.07
T1ρ		4000	+0.14
		5000	+0.15
zg	63		+0.02
CPMG			+0.13
		2000	+0.12
T1ρ		4000	+0.10
		5000	+0.17
zg			+0.02
CPMG			+0.07
	128	2000	+0.08
T1ρ		4000	+0.15
		5000	+0.19

Table SI.4. Width at half height of the creatine singlet (3.03 ppm) [Average over five randomly selected samples]

	$CPMG_{600\mu s}^{416Hz}$	$CPMG_{200\mu s}^{1.25\ kHz}$	$T_{1\rho}^{2kHz}$	$T_{1\rho}^{4kHz}$	$T_{1\rho}^{5kHz}$
WHH	1.06 Hz	1.24 Hz	0.95 Hz	1.09 Hz	1.44 Hz

Table SI.5. The OPLS-DA R^2_Y, Q^2_Y and *p*-values for HFS vs. C serum samples.

A	N = 18	R^2_Y	Q^2_Y	*p*-value
1+1+0	CPMG	0,887	0,678	0,0034
1+1+0	$T^{2kHz}_{1\rho}$	0,898	0787	0,00027
1+1+0	$T^{4kHz}_{1\rho}$	0,854	0,645	0,0062
1+1+0	$T^{5kHz}_{1\rho}$	0,886	0,737	0,00098

Table SI.6. $R_{1\rho}$ (s⁻¹) evolution of some chosen metabolites, from liver sample C3, randomly chosen, as a function of spinning (ν_R) and nutation (ν_1) frequency.

Metabolites ／ ν_1 (Hz)	ν_R = 1000 Hz					ν_R = 4000 Hz				
	6000 Hz	5000 Hz	4000 Hz	3000 Hz	2000 Hz	6000 Hz	5000 Hz	4000 Hz	3000 Hz	2000 Hz
β-D-Glucose Doublet	4,92	4,95	4,88	4,89	4,83	11,84	7,07	5,03	6,49	9,05
Creatine Singlet	5,38	5,54	5,81	5,89	6,22	5,66	5,95	6,19	6,85	6,45
Glycerophosphocholine Singlet	2,64	2,29	2,64	2,33	2,56	5,06	5,19	5,47	5,85	31,32
Choline Singlet	6,63	6,99	7,302	7,72	8,28	4,70	4,63	4,59	5,12	35,39
Alanine Doublet	6,11	6,07	6,15	6,28	6,98	7,35	7,66	8,56	9,32	27,91
Lactate Doublet	8,27	8,97	9,42	10,07	11,95	16,35	16,92	19,31	18,83	17,09

$R_{1\rho}$ evolution of some chosen metabolites, from liver sample C3, as a function of spinning rate (ν_R) for (ν_1 = 4 kHz)

	ν_R = 1000 Hz	ν_R = 4000 Hz	$R_{1\rho}$ evolution
β-D-Glucose Doublet	4,88	5,03	↑
Creatine Singlet	5,81	6,19	↑
Glycerophosphocholine Singlet	2,64	5,47	↑
Choline Singlet	7,302	4,59	↓
Alanine Doublet	6,15	8,56	↑
Lactate Doublet	9,42	19,31	↑

Figure SI.7. T_2- and $T_{1\rho}$-edited spectra for three samples taken from the same control liver, sample C2. (A) CPMG, (B) $T_{1\rho}$, (C) PROJECT. In red the spectra acquired at $v_R = 4000$ Hz, in blue at $v_R = 1000$ Hz.
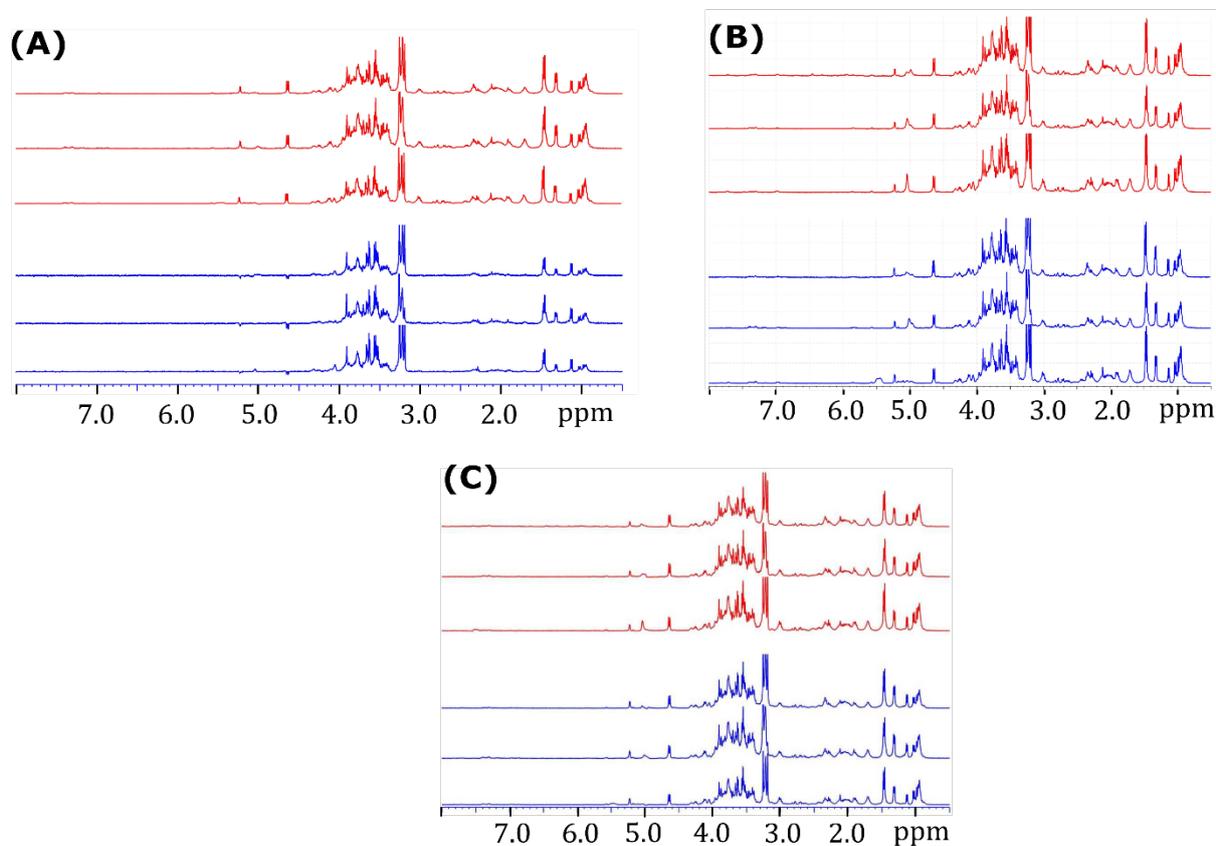

Figure SI.8. OPLS-DA score plots performed on all liver samples including the two groups C and HFS obtained for each sequence (CPMG vs. PROJECT vs. $T_{1\rho}$) at $v_r = 4$ kHz (**a**) and $v_r = 1$ kHz (**b**).
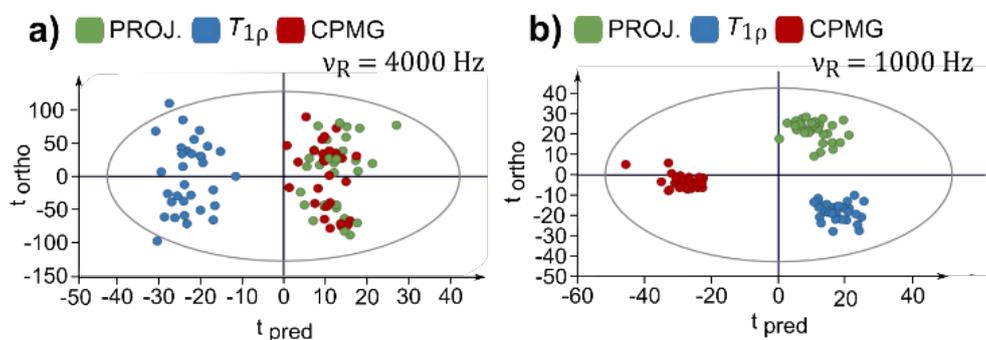
Table SI.9. The OPLS-DA R^2_Y, Q^2_Y and *p*-values for HFS vs. C samples of livers without one outlier (with N = number of the samples and A = number of components to fit the model) using UV scaling.

	N	A	R^2_Y	Q^2_Y	*p*-value
ν_r =1000 Hz					
CPMG	17	1+1+0	0,966	0,770	0,00083
$T_{1\rho}$	17	1+1+0	0,869	0,673	0,0062
PROJECT	17	1+1+0	0,857	0,650	0,0090
ν_r = 4000 Hz					
CPMG	17	1+1+0	0,947	0,798	0,00039
$T_{1\rho}$	17	1+1+0	0,923	0,793	0,00045
PROJECT	17	1+1+0	0,943	0,797	0,00041

Table SI.10. Results of serum biochemical analysis and body weight after 10 weeks of diet. Table duplicate from [33]. Data of an additional group (HFS + C) are added to illustrate the increase in standard deviation by the introduction of an external factors: HFS dietary imbalance, then HFS + C supplementation (or medication). The heterogeneity of the response to each stimuli results in an increase in the standard deviation.

HFS high fructose and saturated fatty acids, C curcuma (administration of hydroalcoholic extract of tumeric 100 mg/kg/day). Relative liver weight is defined as liver weight divided by body weight. Values are mean ± S.E.M (n = 6-12 rats/group).

Group	Controls	HFS	HFS+C
Body Weight (g)	435.17 ± 20.74	438.42 ± 31.85	444.75 ± 50.78
Gain Weight (g)	245.16 ± 8.47	248.42 ± 9.19	254.75 ± 14.66
Relative liver weight	0.0262 ± 0.00078	0.0310 ± 0.0010 **	0.0334 ± 0.0016 **
HOMA-IR	1 ± 0.33	10.79 ± 1.89 **	6.97 ± 2.05 *
Insulin (µg/l)	0.48 ± 0.13	3.34 ± 0.50 *	2.22 ± 0.69 *
Glucose serum (g/l)	1.07 ± 0.185	1.82 ± 0.41 *	1.80 ± 0.44 *
Total cholesterol serum (g/l)	0.60 ± 0.02	0.68 ± 0.04 *	0.66 ± 0.06
Triglycerides serum (g/l)	0.435 ± 0.15	0.878 ± 0.22 *	1.114 ± 0.36 *

*P < 0.05 vs. the control
**P < 0.01 vs. the control.

HOMA-IR: Homeostasic Model Assessment of insulin resistance.

Figure SI.11. Multivariate analysis using OPLS-DA performed on liver samples for the two groups: C and HFS obtained for each sequence: CPMG (a), $T_{1\rho}$ (b) and PROJECT (c), at $v_r = 1$ kHz.
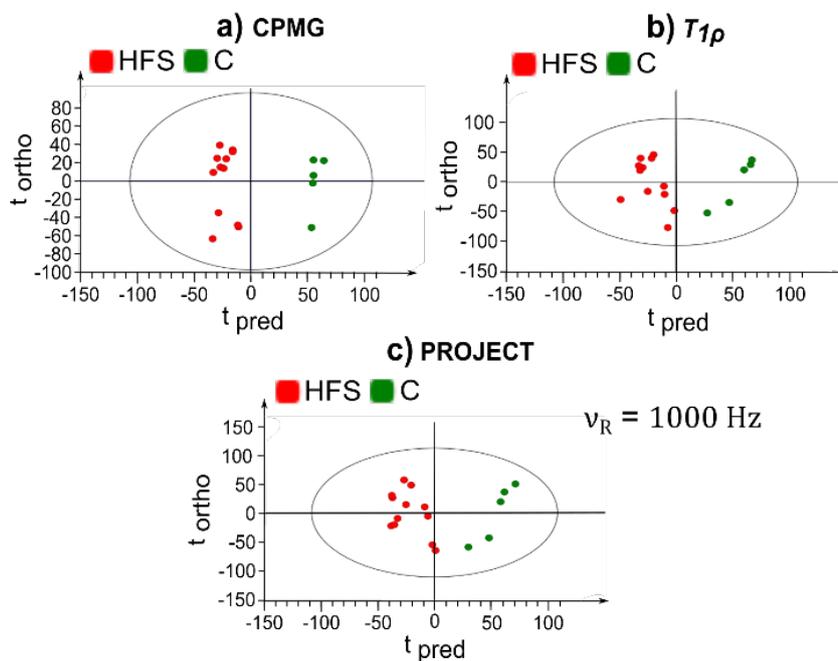
Figure SI.12. S-line plots of the OPLS-DA models of **Figure SI.10.** for CPMG, $T_{1\rho}$, PROJECT at ν_R = 1000 Hz for liver samples.
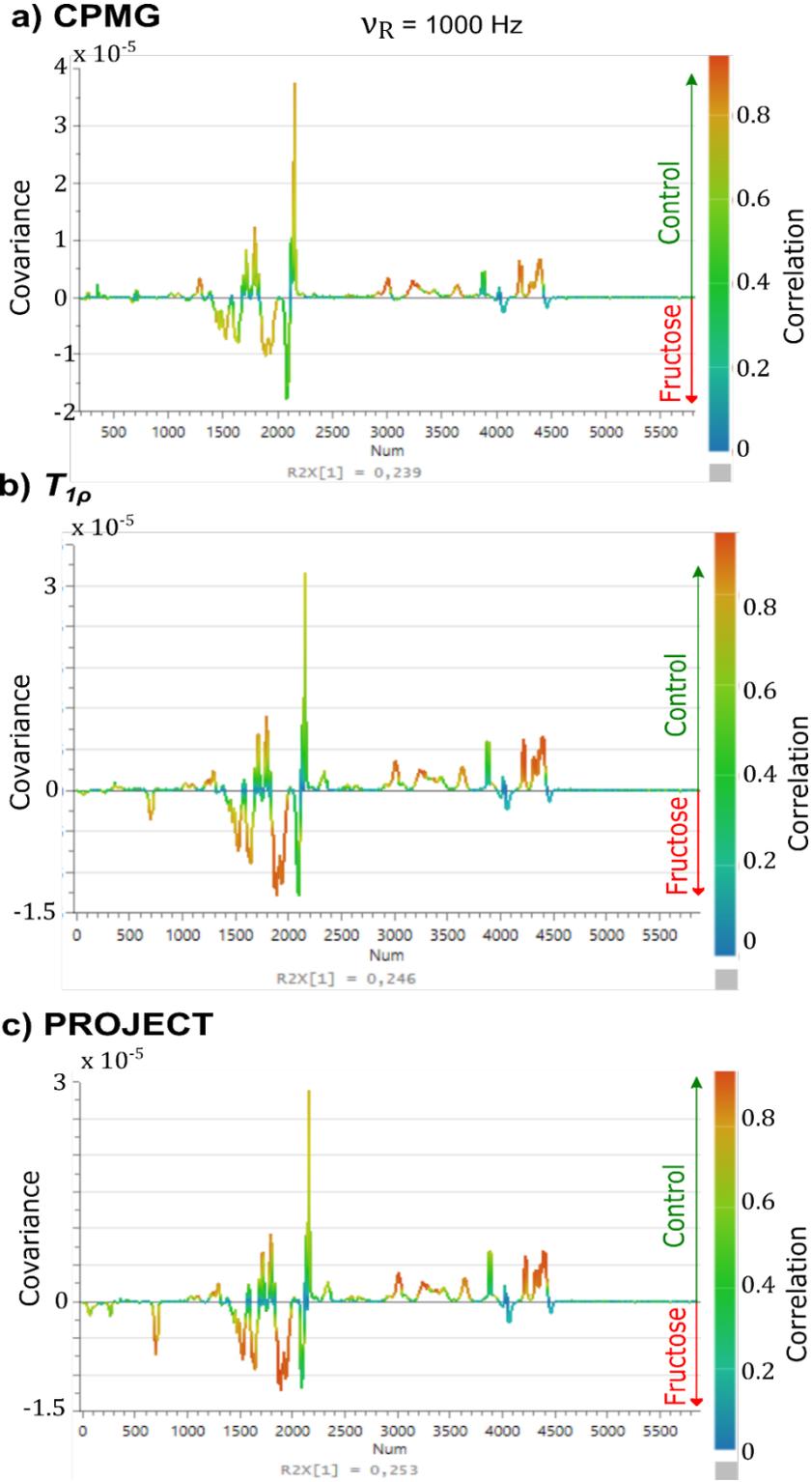
Figure SI.13. S-line plots of the OPLS-DA models of **Figure SI.11.** for CPMG, T1ρ, PROJECT at ν_R = 4000 Hz for liver samples.